

**Key Points:**

- Higher temporal meteorological resolution increases wind stress acting on the sea surface and water column turbulent kinetic energy
- Consequently, a shorter stratified period occurs, resulting in a shorter growing season and delayed onset of the phytoplankton bloom
- Differences in resource limitations across sites may determine the response in ecosystem dynamics to changing meteorological resolution

**Supporting Information:**

- Supporting Information S1

**Correspondence to:**

H. R. Powley,  
hpo@pml.ac.uk

**Citation:**

Powley, H. R., Bruggeman, J., Hopkins, J., Smyth, T., & Blackford, J. (2020). Sensitivity of shelf sea marine ecosystems to temporal resolution of meteorological forcing. *Journal of Geophysical Research: Oceans*, 125, e2019JC015922. <https://doi.org/10.1029/2019JC015922>

Received 4 DEC 2019

Accepted 10 MAY 2020

Accepted article online 16 MAY 2020

©2020. The Authors.

This is an open access article under the terms of the Creative Commons Attribution License, which permits use, distribution and reproduction in any medium, provided the original work is properly cited.

# Sensitivity of Shelf Sea Marine Ecosystems to Temporal Resolution of Meteorological Forcing

Helen R. Powley<sup>1</sup> , Jorn Bruggeman<sup>1</sup> , Jo Hopkins<sup>2</sup> , Tim Smyth<sup>1</sup> , and Jerry Blackford<sup>1</sup> 

<sup>1</sup>Plymouth Marine Laboratory, Plymouth, UK, <sup>2</sup>National Oceanography Centre, Liverpool, UK

**Abstract** Phytoplankton phenology and the length of the growing season have implications that cascade through trophic levels and ultimately impact the global carbon flux to the seafloor. Coupled hydrodynamic-ecosystem models must accurately predict timing and duration of phytoplankton blooms in order to predict the impact of environmental change on ecosystem dynamics. Meteorological conditions, such as solar irradiance, air temperature, and wind speed are known to strongly impact the timing of phytoplankton blooms. Here, we investigate the impact of degrading the temporal resolution of meteorological forcing (wind, surface pressure, air, and dew point temperatures) from 1–24 hr using a 1-D coupled hydrodynamic-ecosystem model at two contrasting shelf-sea sites: one coastal intermediately stratified site (L4) and one offshore site with constant summer stratification (CCS). Higher temporal resolutions of meteorological forcing resulted in greater wind stress acting on the sea surface increasing water column turbulent kinetic energy. Consequently, the water column was stratified for a smaller proportion of the year, producing a delayed onset of the spring phytoplankton bloom by up to 6 days, often earlier cessation of the autumn bloom, and shortened growing season of up to 23 days. Despite opposing trends in gross primary production between sites, a weakened microbial loop occurred with higher meteorological resolution due to reduced dissolved organic carbon production by phytoplankton caused by differences in resource limitation: light at CCS and nitrate at L4. Caution should be taken when comparing model runs with differing meteorological forcing resolutions. Recalibration of hydrodynamic-ecosystem models may be required if meteorological resolution is upgraded.

**Plain Language Summary** Computer models are used to predict the impact of changes in environmental pressures such as climate change on marine ecosystems. To predict these changes models need to accurately simulate the period when marine plants (phytoplankton) grow rapidly, termed the phytoplankton bloom, as these plants act as a food source to the marine food chain. The models are run by defining meteorological variables, such as light, air temperature, and wind speed, which are known to strongly impact the timing of phytoplankton blooms. In this paper we investigate the impact in changing the time period between inputs of meteorological variables from 1 to 24 hr at two contrasting marine sites. The shorter the time span between inputs, the more fluctuations in wind speed, resulting in increased wind stress acting on the sea surface and therefore greater turbulence and mixing within the water column. Consequently, the predicted length of growing season is reduced with the spring phytoplankton bloom starting up to 6 days later and the autumn bloom often terminating earlier. Implications for ecosystem function are site dependent. Caution should be taken when comparing model results using different time gaps of meteorological inputs and models may need retuning if upgraded to hourly meteorological inputs.

## 1. Introduction

Phytoplankton phenology, that is, the timing of phytoplankton blooms, has consequences that cascade through ecological trophic levels, with the potential to change ecosystem structure (Edwards & Richardson, 2004; Platt et al., 2003) and the flux of carbon to the sea floor. This is particularly important in shelf seas as they trap a disproportionate amount of carbon from the atmosphere within their sediments compared to the deep global ocean (Bauer et al., 2013; Sharples et al., 2019). The ability of marine ecosystem models to accurately represent and capture changes in phytoplankton phenology, in addition to the magnitude and composition of phytoplankton blooms, is imperative to predict the impacts of environmental change on ecosystem dynamics and the amount of carbon trapped within global shelf seas.

Phytoplankton blooms occur when an optimal set of environmental conditions, in particular nutrient and light availability, both of which are mediated by turbulent mixing, support growth rates that exceed losses

(e.g., grazing). There are several competing theories regarding the causes of the onset of the spring bloom. The critical depth theory (Sverdrup, 1953) states that phytoplankton blooms will develop when the mixed layer is less than the critical depth: The depth where vertically integrated phytoplankton growth exceeds phytoplankton losses. In more recent years, at least two other hypotheses have been formulated. The critical turbulence theory postulates that a phytoplankton bloom can occur in unstratified waters if turbulent mixing is weak enough that phytoplankton stay within the photic zone long enough to photosynthesize (Huisman et al., 1999; Taylor & Ferrari, 2011), while the disturbance-recovery hypothesis (Behrenfeld, 2010; Behrenfeld et al., 2013) states that the phytoplankton bloom is dependent on the balance of phytoplankton loss and production due to grazing pressures and physical properties. On shelves where light rather than nutrient availability limits phytoplankton growth, the spring bloom typically occurs during a period of low grazing pressure when a reduction in turbulent mixing and shoaling of the actively mixing surface layer eases light limitation.

In contrast to the spring bloom, the autumn phytoplankton bloom typically occurs when light is still non-limiting and is fueled by entrainment of nutrients into the euphotic zone as convection and wind mixing deepen the surface mixed layer. In addition, the phytoplankton composition within the autumn bloom is different to that of spring: More motile species are present that have the ability to migrate across the mixed layer between nutrient rich and nutrient poor regions of the water column (Smyth et al., 2014). Although not studied as intensively as the spring phytoplankton bloom, the autumn phytoplankton bloom can also make a substantial contribution to annual gross primary production (Wihsgott et al., 2019).

In all hypotheses for phytoplankton bloom initiation, the timing of the phytoplankton bloom is closely coupled to meteorological indices such as light, temperature, and wind speeds. Wind and temperature alter the timing of stratification events in spring and autumn and the strength of stratification in summer, in addition to the amount of turbulent kinetic energy present throughout the water column. Chiswell (2011) links the timing of the spring bloom to a reduction in wind-driven surface mixing with wind intensity estimated to explain up to 60% of the interannual variability in the timing of phytoplankton blooms along the Norwegian shelf (Vikebø et al., 2019). Changing wind conditions have also been shown to both advance and delay the onset of spring phytoplankton blooms (Follows & Dutkiewicz, 2002; Ruiz-Castillo et al., 2019; Sharples et al., 2006; Waniek, 2003). A decrease in wind stress is often correlated with an earlier phytoplankton bloom in open oceans such as in the Japan Sea (Kim et al., 2007; Yamada & Ishizaka, 2006), North Atlantic (González Taboada & Anadón, 2014; Henson et al., 2009; Ueyama & Monger, 2005), the open ocean off the South West Iberian peninsula (Krug et al., 2018), and shallower systems such as the North West European Shelf (González Taboada & Anadón, 2014) and Baltic Sea (Groetsch et al., 2016). However, in the shelf region off the South West Iberian peninsula and at Station L4 in the English Channel, an increase in wind speeds was linked to increased chlorophyll peaks and earlier bloom starts due to relief of nutrient stress (Barnes et al., 2015; Krug et al., 2018). Winds have also been highlighted as important in influencing the autumn bloom by breaking down stratification enabling nutrients to reach the surface (Kim et al., 2007; Wihsgott et al., 2019).

Hydrodynamic-ecosystem models are forced by meteorological data. It has long been recognized that temporal meteorological resolution within these models impacts ecosystem dynamics (Backhaus, 1985; Pohlmann, 1996b; Ridderinkhof, 1992). In particular, low temporal and spatial resolution meteorological data may miss short-lived events, especially in wind speed or cloud cover, which could be important for phytoplankton phenology and consequently ecosystem dynamics. Pre-1980s annual or monthly mean atmospheric forcing variables were used in hydrodynamic-ecosystem models until Backhaus (1985) recognized that variable wind fluxes have large influences on surface currents in shelf sea regions (Pohlmann, 1996b). In response, the early versions of the European Regional Seas Ecosystem Model (ERSEM) used observationally derived meteorological data on a 3- to 6-hourly timescale (i.e., Lenhart et al., 1995, 1997; Pohlmann, 1996a). However, these data have the caveat that as they are buoy/station based, they are only available at specific sites resulting in a coarse spatial resolution. The production of atmospheric reanalysis products, such as ones by the European Centre for Medium range Weather Forecasting (ECMWF) and National Centre for Environmental Prediction (NCEP) increased the spatial resolution of available meteorological data and thus the ability to model larger areas. Consequently, the temporal resolution of atmospheric forcing data used to force ERSEM since the mid-1990s has varied from monthly to hourly resolution (i.e., Aveytua-Alcázar et al., 2008; Blackford, 2002; Blackford & Burkill, 2002; Holt &

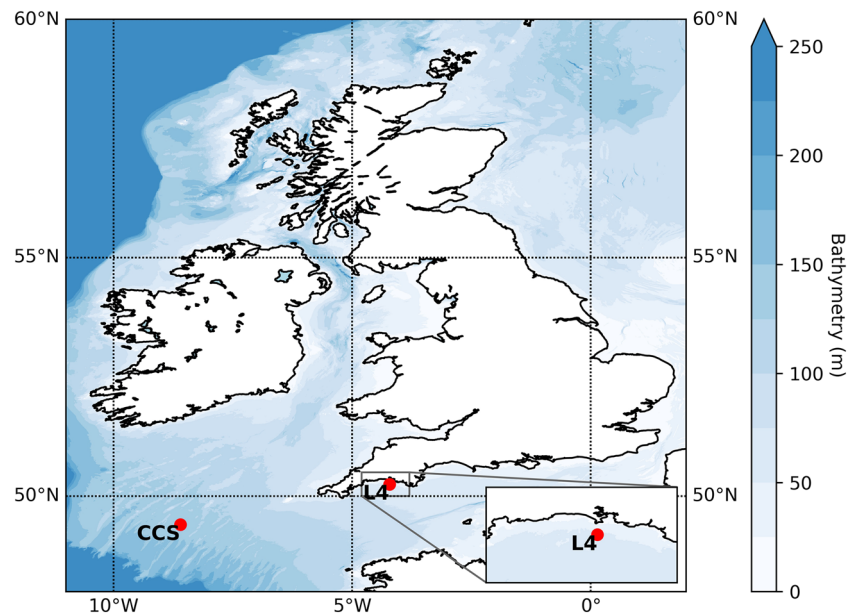


**Figure 1.** Map of station locations. Colors represent bathymetry (GEBCO\_2019 grid, www.gebco.net).

James, 2001; Raick et al., 2005; Siddorn et al., 2007; Vichi et al., 1998) depending on the source of the meteorological data. The release of the publicly available globally resolved hourly datasets from the ECMWF (ERA5; C3S, 2017) and NCEP (CFSR; Saha et al., 2010, 2014) will result in an increase in the temporal resolution of the meteorological forcing in hydrodynamic ecosystem models, potentially impacting both phytoplankton phenology and ecosystem dynamics.

This paper investigates the impact of meteorological forcing on phytoplankton phenology and ecosystem dynamics within shelf seas. We use a 1-D hydrodynamic-ecosystem model to allow multiple simulations with the temporal resolution in meteorological forcing decreasing from 1 to 24 hr. The model is run at two contrasting seasonally stratified shelf sea sites: the coastal L4 station in the western English Channel (Smyth et al., 2010, 2015) and at a site in the more isolated Central Celtic Sea (CCS). Changes in the physical dynamics of the water column and subsequent phytoplankton phenology between the different scenarios are assessed. Results are put into context of the impact to the global carbon cycle and the differences in the responses of the two stations are investigated.

## 2. Methods

### 2.1. Site Locations and Observations

L4 is part of the Western Channel Observatory, located 13 km offshore from Plymouth, UK (50.25°N, 4.2167°W; Figure 1). It represents a seasonally stratified coastal system with a depth of 50 m and is influenced by riverine inputs from the Tamar and Plym rivers. Observational data have been collected at L4 on a weekly basis since 1988. The time series initially consisted of sea surface temperature, zooplankton, and phytoplankton data and was later supplemented with CTD profiles and nutrient data among others, in the early 2000s (Smyth et al., 2015). In contrast, the CCS station represents a seasonally stratified open shelf system. It is situated in the CCS near the edge of the North West European Shelf 220 km southwest of Land's End, UK (49.4°N, 8.6°W; Figure 1). It has a depth of 145 m and was the focus of an intense physical, chemical, and biological sampling campaign during the Shelf Sea Biogeochemistry project between 2014 and 2015 (Sharples et al., 2019). Observational data were obtained from the British Oceanographic Data Centre (BODC: www.bodc.ac.uk) for both L4 (Fishwick, 2018; Woodward & Harris, 2019) and CCS (Cruises JC105, DY026, DY018, DY021, DY029, DY030, DY033, and DY034; Hull et al., 2017; Wihsgott et al., 2016; E. M. S. Woodward, 2016; M. Woodward, 2016).

## 2.2. Hydrodynamic-Ecosystem Model

Here, ERSEM (Butenschön et al., 2016) is coupled to the 1-D General Ocean Turbulence Model (GOTM; Burchard et al., 1999) using the Framework for Aquatic Biogeochemical Model (FABM; Bruggeman & Bolding, 2014). ERSEM is a high complexity lower trophic food web model including both pelagic and benthic systems. It represents the biogeochemical cycling of five elements (carbon, nitrogen, phosphorus, silicon, and oxygen) modulated by the cycling between producers, consumers, and decomposers using variable stoichiometric ratios. ERSEM uses a functional group approach further partitioning each set using trait and size to form four phytoplankton groups, three zooplankton groups, and one bacteria group within the pelagic model. In addition, various sizes and reactivities of particulate organic matter and dissolved organic matter are included as state variables within the pelagic model along with five inorganic nutrient groups. The pelagic model is coupled to a benthic model containing particulate and dissolved organic matter, deposit feeders, suspension feeders, meiofauna, anaerobic and aerobic bacteria, and inorganic nutrients.

The model is configured to simulate a time period covering 2008 to 2015. Model results are reported for 2010–2015 with the first 2 years of the simulation considered the model spin up. Note that the CCS simulation finishes in August 2015 due to a lack of temperature and salinity data beyond this time period. Thus, at CCS, results for spring 2015 are included within results presented in this paper but annual results are not included for 2015. The model is run with 100 vertical levels ranging from a minimum thickness of 6 and 18 cm near the surface, at L4 and CCS respectively, to a maximum of 87 and 252 cm in the middle of the water column. Sensitivity tests show that differences in vertical resolution between the sites have minimal impact on model results (results not shown). All model outputs are saved as daily means.

## 2.3. Site Specific Setup—“Baseline” Model

Tidal forcing data were provided to GOTM using hourly depth-averaged horizontal velocities and sea surface elevations at both sites (Cazenave et al., 2016). Hourly meteorological variables (10 m zonal ( $u$ ) and meridional ( $v$ ) components of wind, sea surface pressure, 2 m air temperature, 2 m dew point temperature, total cloud cover, precipitation, and net shortwave radiation) for the time period 2008–2016 were extracted from the ERA5 reanalysis data set (C3S, 2017), which is provided at a spatial resolution of  $0.25^\circ \times 0.25^\circ$ . Meteorological variables were linearly interpolated to each site location. Due to forcing the model with hourly *net* shortwave radiation, surface reflectance within GOTM was disabled.

This study uses the 1-D L4 setup provided as a test case in ERSEM 16.05 (Butenschön et al., 2016) as the baseline model from which changes as outlined below and in Table S1 were made. The 1-D model at both sites is relaxed on a yearly timescale to observed temperature and salinity data (Fishwick, 2018; Wihsgott et al., 2016) to avoid drift in these variables during the model run. Note that this means the influence of changes in river flow on salinity at L4 and CCS, and thus stratification, is not included in the model simulations. No relaxation was applied to any biogeochemical variables at either site. Model calibration at CCS was performed with the aim of changing the minimum number of parameters from the basic L4 setup as possible.

The model at CCS is initialized using average winter nutrient concentrations over 2014 and 2015 (BODC, E. M. S. Woodward, 2016). The benthic model at CCS was spun up so that a quasi-steady state was achieved—this allowed only a 2 year model spin-up period at the start of each model run. For L4 the published parameter set was assumed to provide a quasi steady state. To prevent the increase of benthic particulate matter and benthic refractory organic matter at both L4 and CCS, the affinity of benthic aerobic and anaerobic bacteria to benthic particulate organic matter was increased to  $4 \times 10^{-5} \text{ m}^2 (\text{mg C})^{-1} \text{ day}^{-1}$ , and affinity to benthic refractory organic matter to  $4 \times 10^{-6} \text{ m}^2 (\text{mg C})^{-1} \text{ day}^{-1}$  (Table S1 in the supporting information). The  $k$  epsilon turbulent scheme was used within GOTM for both sites with the minimum turbulent kinetic energy ( $k_{\text{min}}$ ) at both sites increased to match temperature profiles with observations. The absorption of silt was lowered at the CCS site to improve timing of the phytoplankton bloom and depth of subsurface chlorophyll maximum in summer within the model relative to observations (Hopkins et al., 2019). The nitrification rate constant was also lowered at both sites to improve ammonium dynamics at depth. Finally, the wind speed relative to current velocity, rather than the default setting of absolute wind speed, was used to calculate air-sea fluxes. Both models were validated with observational data using robust statistics. Target diagrams showing bias, mean absolute error (MAE) and correlation coefficient (Butenschön et al., 2016; Jolliff et al., 2009) can be found in the supplementary material (Figure S1).



#### 2.4. Meteorological Resolution Forcing Scenarios

Meteorological forcing scenarios were created using the instantaneous meteorological data, that is, 10 m  $u$  and  $v$  components of wind, sea surface pressure, 2 m air temperature, 2 m dew point temperature, and total cloud cover. Throughout this paper the term “meteorological forcing” refers to these variables. Six-hourly, 12-hourly, and 24-hourly meteorological forcing data were subsampled from the hourly meteorological data to create the forcing scenarios. This sampling method was chosen to reflect the potential changes from switching resolution of meteorological products such as from 6-hourly ERA-Interim data to hourly ERA 5. Precipitation and hourly net short wave radiation were kept at an hourly resolution for all scenarios as these are time-integrated variables that already capture the change throughout the time interval. Thus, while reduction in the time resolution in precipitation and net shortwave radiation causes their variability to be underestimated, it does not affect total heat or freshwater input. In addition, we chose not to adjust the resolution of shortwave radiation as resultant changes in meteorological forcing may be highly dependent on individual model formulations for light and are also hard to disentangle from other effects such as wind and temperature. Conversely, a reduction in resolution of instantaneous variables introduces biases in the mean of the time series of meteorological inputs of up to 3% (in  $u$  and cloud cover) and 0.8% ( $u$ ) at L4 and CCS, respectively, for the scenarios compared to the hourly simulation (Table S2); additionally, reduced variability of some instantaneous variables (e.g., wind speed) will impact energy fluxes. In order to identify which meteorological variables the model was sensitive to, the model was run a further 5 times, dropping one by one the temporal resolution of each individual meteorological forcing variable to 12-hourly, leaving all other variables at hourly resolution.

#### 2.5. Physical/Phenological Indices

Meteorological resolution impacts the average environment (light and nutrients) experienced by phytoplankton through modulation of turbulence, which controls the depth over which phytoplankton are mixed. This is the cornerstone of the critical depth and critical turbulence hypotheses. Throughout this manuscript we use the mixed layer depth (MLD) as an indicator of the depth of near-surface stratification and as an estimate of the depth of the actively mixing surface layer, quantities most relevant to phytoplankton growth in the euphotic zone. We also calculate the potential energy anomaly (Simpson et al., 1981) as a measure of the overall strength of stratification throughout the water column. Typically, a shallower MLD in the spring is associated with an increase in stratification and often corresponds to a temporal shift in the onset of stratification. A deeper MLD frequently represents weakening stratification and often corresponds with a temporal shift in the breakdown of stratification in autumn.

A MLD criteria is used to identify different hydrodynamic-biogeochemical regimes observed throughout the seasons to aid analysis. The MLD is often defined as the depth at which the density changes by 0.03–0.125  $\text{kg m}^{-3}$  from a reference level (de Boyer Montégut et al., 2004, and references therein). Here we defined the MLD as a change in density of more than 0.06  $\text{kg m}^{-3}$  from the 2 m density. The assigned seasons reflect the onset of stratification where the spring bloom occurs and wanes (spring), stable stratification (summer), and the time period where stratification is eroded by a deepening of the mixed layer resulting in nutrients being mixed back into the surface water (autumn). The exact method for defining the time periods is shown in Table S3. All calculations used either 10 day forward or backward running means. The same time period for each regime is used across all years and all scenarios. To define this, the minimum or maximum day of the year over all simulations and all scenarios that fulfilled the criteria in Table S3 were used to delineate the exact start and end of each season in the final analysis. Note that the time periods are slightly different for L4 and CCS.

The phytoplankton bloom duration is typically defined as the time period when chlorophyll exceeds 5% of the annual median (Henson et al., 2009; Krug et al., 2018; Racault et al., 2012, 2017; Sapiano et al., 2012; Siegel et al., 2002) with Siegel et al. (2002), indicating that little difference occurs when the percentage is between 1% and 30%. Here, we define the start of the spring phytoplankton bloom as the first day of the year when depth-integrated chlorophyll is more than 10% of the annual median. The end of the phytoplankton bloom is defined when depth-integrated chlorophyll drops below 10% of the annual median for more than six consecutive days. The bloom duration is the time between the start and end of the bloom. This metric however does not capture the autumn phytoplankton blooms at our two sites. Therefore, we also defined the growing season as the period of time when the 10 day running average of mean water column gross

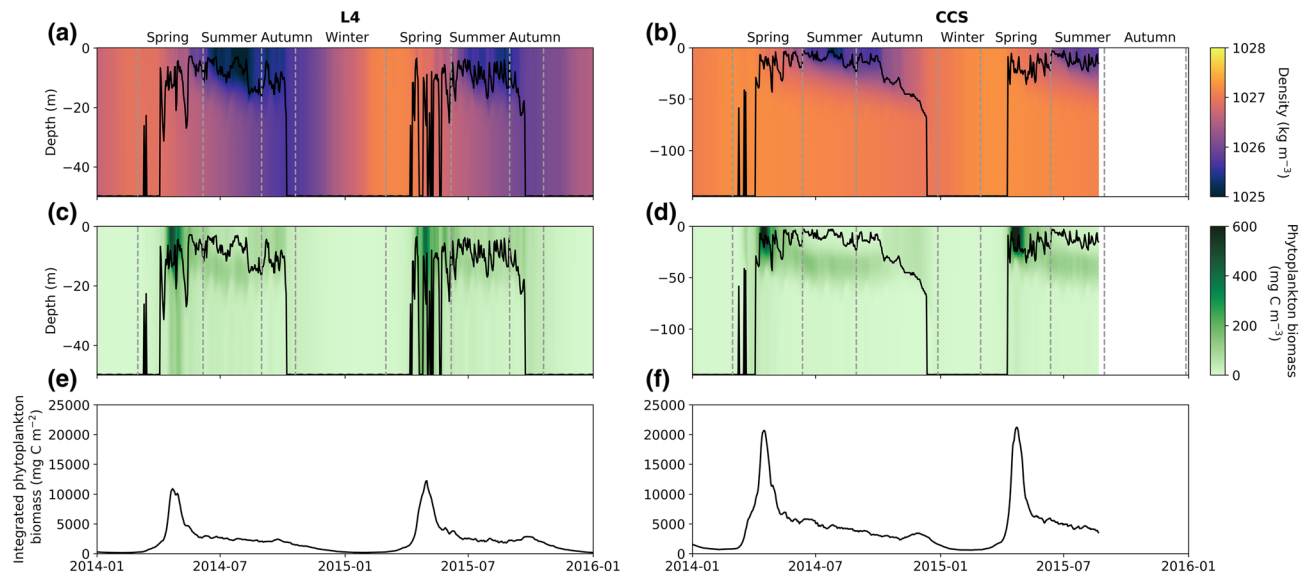


**Figure 2.** Density and phytoplankton biomass distributions at L4 (a, c, and e) and CCS (b, d, and f) in 2014 and 2015. Black line in panels (a)–(d) indicates the mixed layer depth; gray dashed lines delineate seasons. Note difference in depth between L4 and CCS.

primary production (GPP;  $\text{g C m}^{-3} \text{ day}^{-1}$ ) is more than one tenth of the annual maximum GPP at each site. The metrics for chlorophyll and GPP calculated for the hourly simulation are used for all scenarios so that differences between each meteorological scenario can be fairly assessed. Finally, the peak magnitude of the bloom represents the day of the year when depth-integrated chlorophyll is greatest.

### 3. Results

#### 3.1. Sensitivity Tests

The sensitivity tests on individual meteorological variables indicate that changes in the temporal resolution of wind drive differences in physical dynamics between the scenarios presented here at both stations (results not shown). Changing surface pressure, air and dew point temperatures, and cloud cover have minimal impact on phenology and ecosystem dynamics (Figure S2). Thus, throughout the rest of this manuscript, we will focus on the impact of wind in driving ecosystem dynamics.

#### 3.2. Baseline (Hourly) Simulation

The density structure of the water column in the hourly meteorological simulation at both sites in addition to the MLD and assigned seasons for the years 2014 and 2015 are shown in Figure 2. The water column at L4 is well mixed for a longer portion of the year than at CCS. There is also a weaker contrast between surface and bottom water densities during summer at L4 indicating that seasonal stratification is weaker than at CCS. A more intense spring bloom is predicted to occur at CCS and, during the summer, the subsurface chlorophyll maximum is deeper (40 m at CCS compared to 15 m at L4; Figure 2). In addition, a later autumn bloom resulting in a longer growing season is predicted in the model simulation at CCS than at L4 (Figure S3). Comparing near-surface chlorophyll-a concentrations observed at both sites with the baseline model (Figure S3) provides confidence that the simulations are satisfactorily predicting the observed phytoplankton phenology.

#### 3.3. Impacts of Meteorological Resolution on Physical Dynamics

Lower meteorological resolution results in a 2–16% and 2–11% reduction in the annual mean magnitude of wind stress acting on the surface water at L4 and CCS, respectively, between all scenarios and the hourly meteorological simulation (Figure 3). This is a result of missing high intensity short-lived wind events in the coarser, subsampled resolution meteorology. The strong positive relationship between wind stress and depth-integrated turbulent kinetic energy throughout the water column (Figure 3) results in a reduction in turbulent kinetic energy in the scenarios of between 2–12% at L4 and 2–8% at CCS on an annual scale.

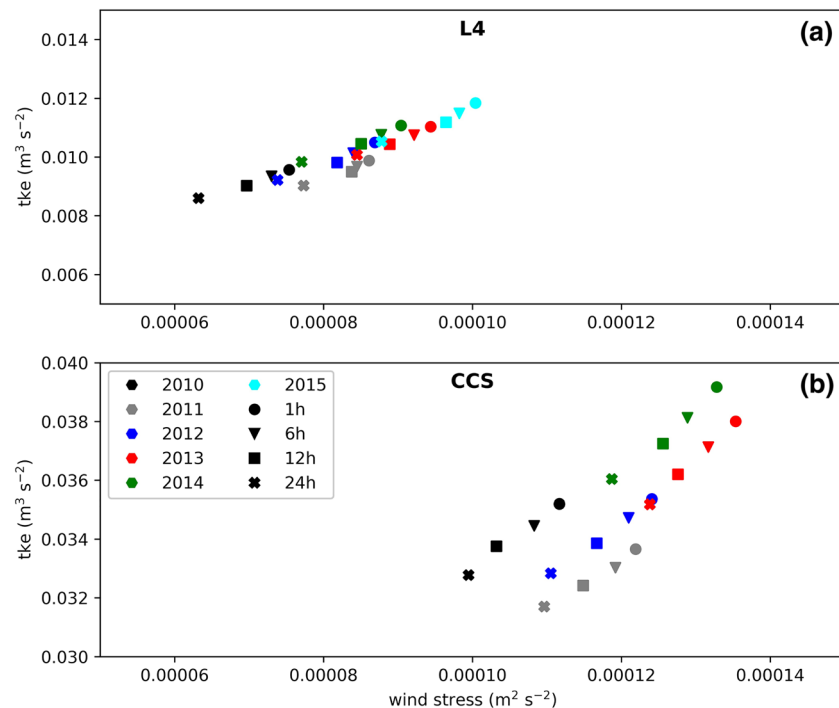


**Figure 3.** (a and b) Correlation between mean annual magnitude of wind stress and mean annual depth-integrated turbulent kinetic energy (tke) for different meteorological forcings (shapes) and individual years (color) between 2010 and 2015.

Tidal forcing dampens the magnitude of change in the response of turbulent kinetic energy to meteorological forcing. Rerunning the model scenarios without tides produces a reduction in turbulent kinetic energy of up to 25% compared to the hourly simulation (4–23% L4; 5–20% CCS; results not shown). The change in turbulent kinetic energy in the upper water column due to meteorological forcing is overwhelmed by the impact of tides throughout the water column. The reduction in turbulent kinetic energy with lower temporal resolution of meteorological forcing gives rise to decreased water column mixing throughout the year resulting in earlier stratification of the water column in spring and later breakdown of stratification in autumn (Figures 4, S4, and S5). Increases in the strength of the stratification as the meteorological resolution is reduced are greater at L4 than at CCS. In addition, the mixed layer becomes increasingly shallower in summer and is up to 3 m thinner at both L4 and CCS in the 24 hr meteorological resolution scenario compared to the hourly simulation.

### 3.4. Change in Phenology

A shift toward an increasingly earlier spring phytoplankton bloom occurs as the temporal meteorological forcing resolution is reduced. The onset of the phytoplankton bloom is up to 4 and 6 days earlier at L4 and CCS respectively in the 24-hourly resolution scenario compared to the hourly simulation (Figure 5a) with similar trends in the timing of peak chlorophyll concentrations (Figure 5g). The trends for the end of the phytoplankton bloom are not as clear as for the onset. On average, the phytoplankton bloom ends later with lowering meteorological resolution resulting in a phytoplankton bloom that is up to 17 and 6 days longer at L4 and CCS, respectively, across all scenarios. However, in some years an earlier and thus shorter bloom occurs at L4 in the scenarios compared to the hourly resolution. The peak magnitude of depth-integrated chlorophyll as the meteorological resolution is reduced is up to 15% and 10% lower than the hourly resolution simulation at L4 and CCS respectively, although occasionally up to a 5% greater magnitude in chlorophyll concentration does occur (Figure 5h).

The weaker trend in the change in the peak amplitude of the bloom to meteorological forcing than other phenological indicators is likely due to the opposing impacts of wind stress on phytoplankton blooms. In some years, differences in the MLDs due to changes in wind stress stimulates a higher magnitude bloom

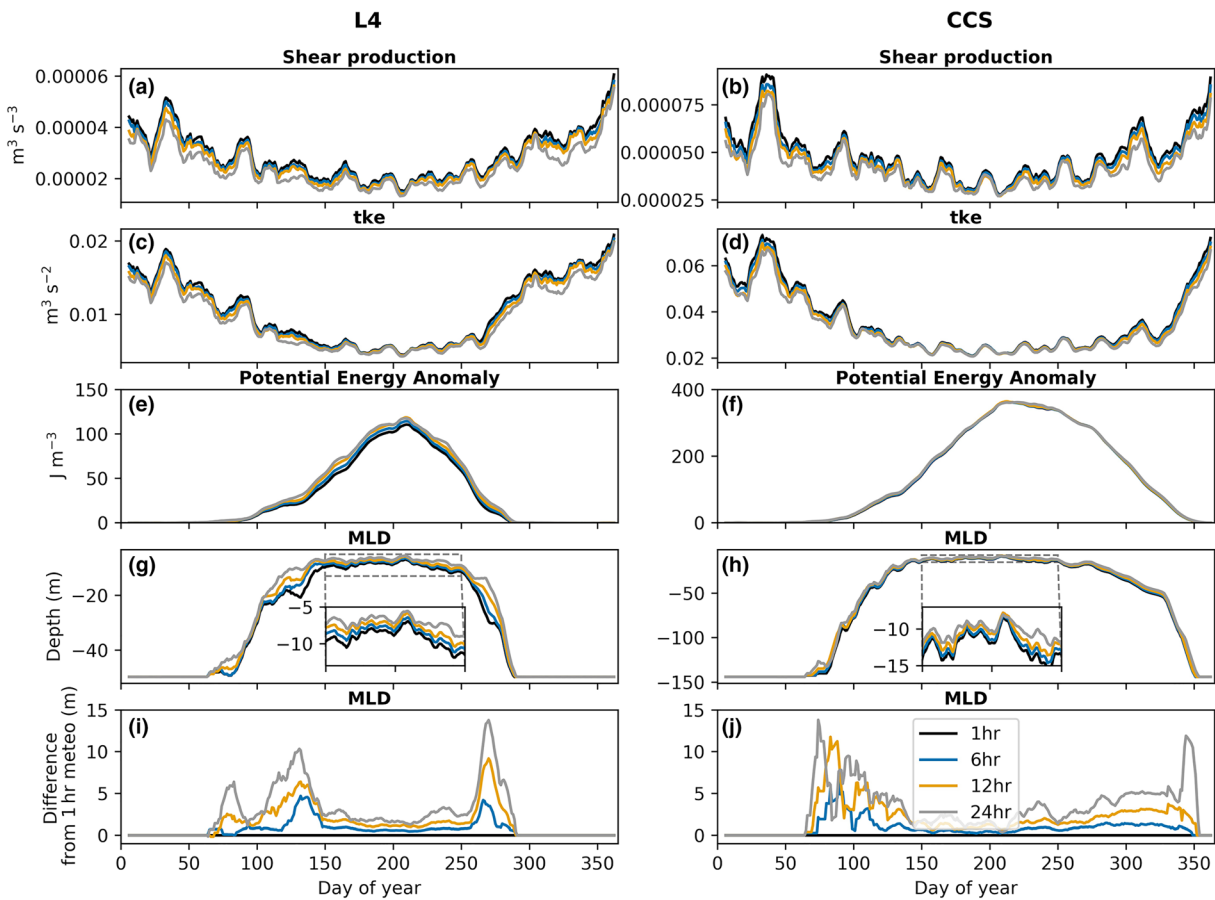


**Figure 4.** Impact of meteorological forcing on physical dynamics baseline hourly simulation and 6-, 12-, and 24-hourly scenarios (a–h), presented as a climatology for the time period 2010 to 2015 calculated using a 10 day running mean. Panels (i) and (j) represent the difference in mixed layer depth (MLD) in the 6, 12, and 24 hr scenarios compared to the hourly simulation with positive values indicating a shallower mixed layer depth. Results for individual years can be found in the supplementary material. tke = turbulent kinetic energy, MLD = mixed layer depth. The potential energy anomaly (Simpson et al., 1981) represents strength of stratification. Note difference in y scales between graphs.

in the hourly meteorological forcing compared to the lower resolution scenarios (i.e., 2014, L4; Figure S5a) due to additional nutrients being mixed into the photic zone. However, occasionally a large wind induced mixing event in the hourly simulation relative to the lower resolution of meteorological forcing may cause the cessation of the bloom due to phytoplankton being mixed down to low light environments and hence produce lower peak chlorophyll concentrations (i.e., 2015 L4; Figure S5a).

### 3.5. Change in Length of Growing Seasons

The increasingly longer period of stratification with lower meteorological resolution supports an increasingly longer growing season of phytoplankton (Figure 5). The start of the growing season is up to 10 days earlier in the 24 hr scenario at L4 and 11 days earlier at CCS compared to the hourly simulation. The end of the growing season is up to 13 and 10 days later at L4 and CCS respectively, although there is little change in the end of the growing season between the hourly and 6-hourly scenario at L4. The overall effect of reducing meteorological resolution at both sites is to increase the growing season by up to 23 days at L4 and 11 days at CCS.

### 3.6. Annual Changes in Carbon Reservoirs

Substantial interannual variability exists in the dynamics of the spring bloom relative to meteorological forcing, and this is demonstrated in the response of carbon stocks (Figure 6). At L4, bacteria and dissolved organic carbon (DOC) biomasses increase with coarsening meteorological resolution, with up to 3% greater biomass in the 24 hr scenario than the hourly simulation, while dissolved inorganic carbon (DIC),



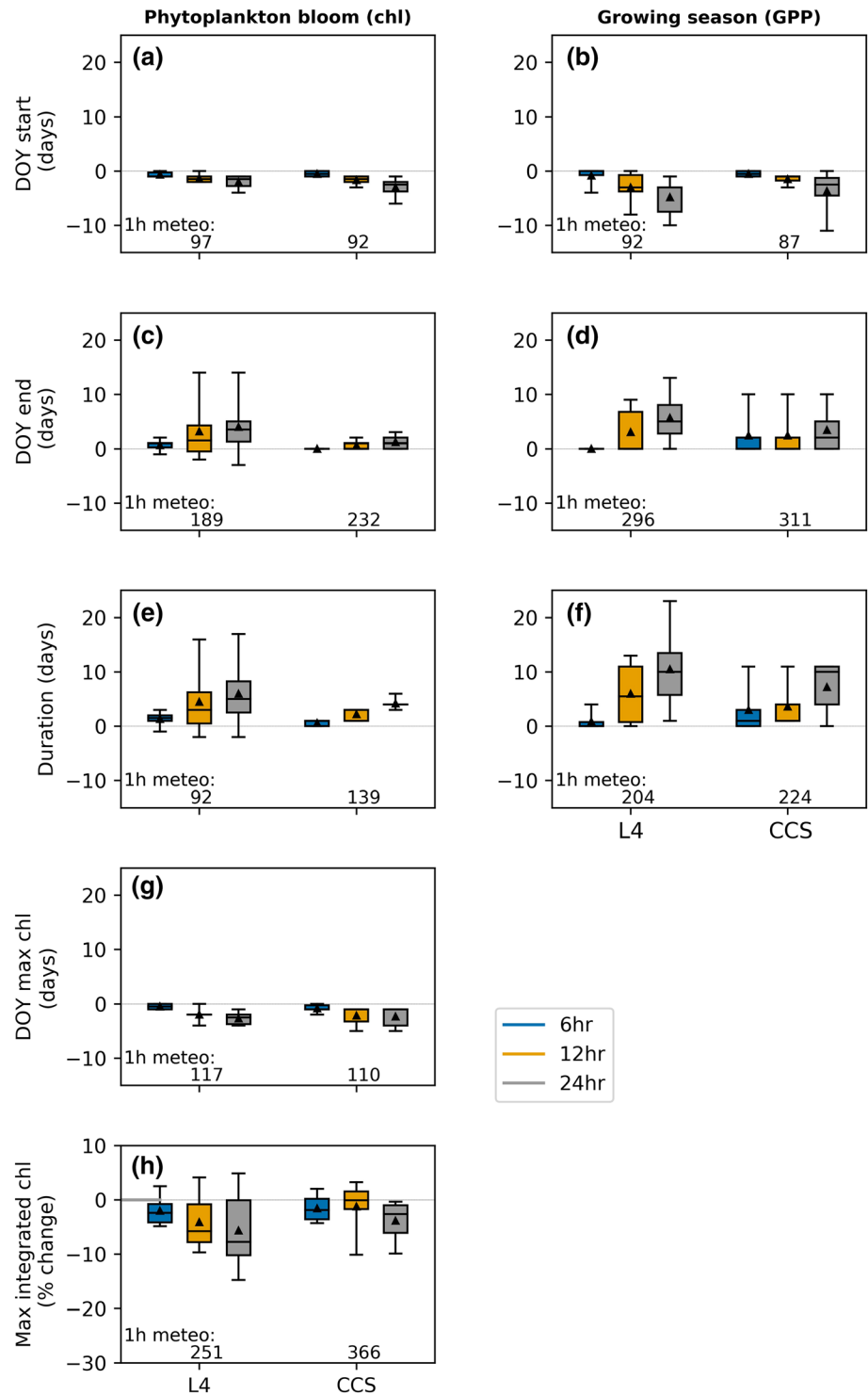


**Figure 5.** Difference in phytoplankton bloom (a, c, e, g, and h) and growing season characteristics (b, d, and f) between 6, 12, and 24 hr scenarios and hourly meteorological resolution simulation at L4 and CCS for each year between 2010 and 2015. For CCS, 2015 results were not included in metrics for day of the year (DOY) end and duration as the model simulation ended in August 2015. Lines through middle of box plots represent median, black triangles: mean, whiskers represent the maximum and minimum range of the data. Numbers on bottom of graph indicate the mean result of the 1 hr meteorological forcing simulation. See text for details on methods used to calculate phytoplankton bloom and growing season statistics. Note the change in y scale in panel (h). chl = chlorophyll-a, GPP = gross primary production.

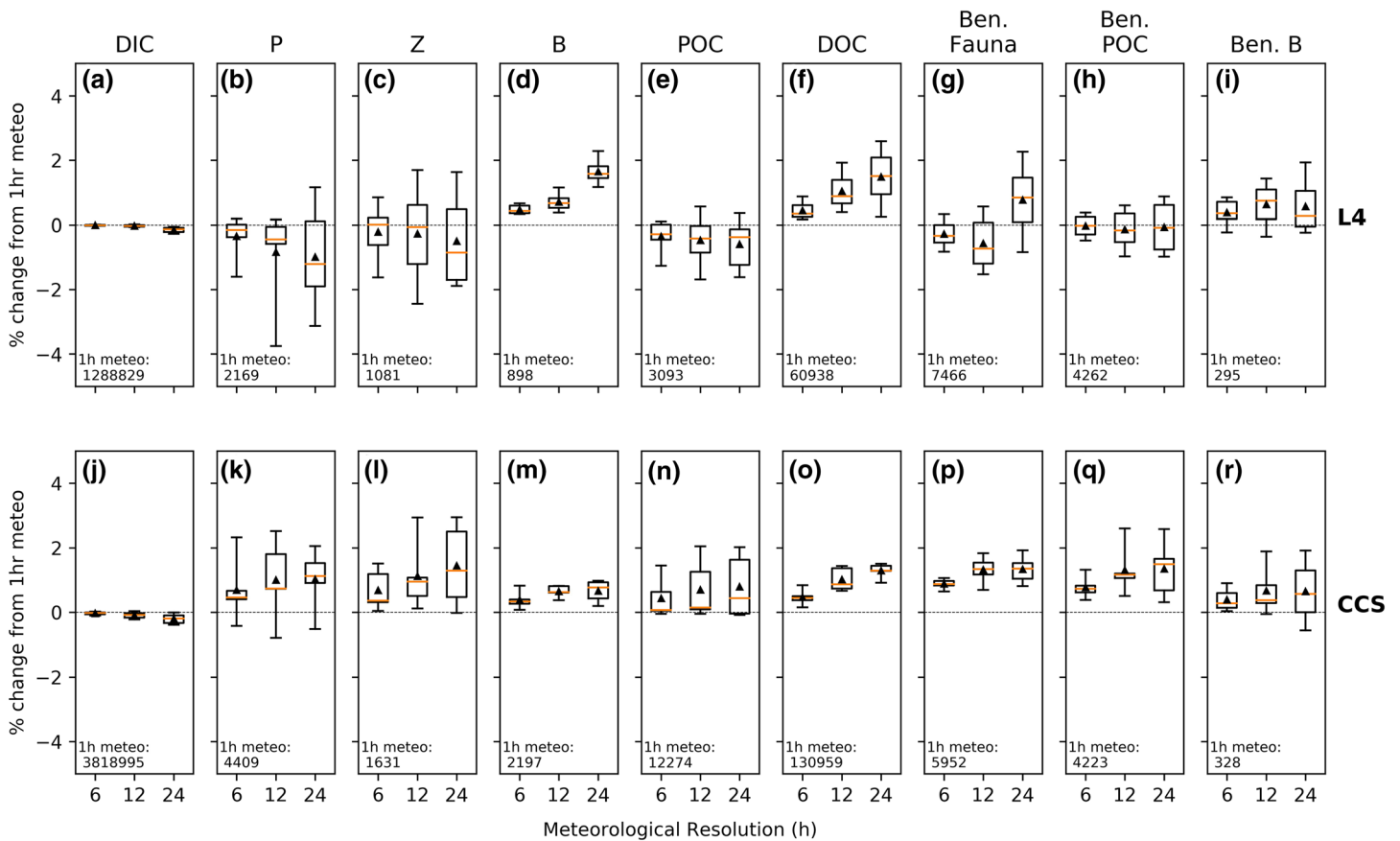


**Figure 6.** Percentage change in the annual distribution of depth-integrated mean carbon biomass for 6-, 12-, and 24-hourly resolutions of meteorological forcing relative to hourly meteorological forcing for each year between 2010 and 2015 at L4 (a–i) and CCS (j–r). For CCS, 2015 results were not included as the model simulation ended in August 2015. Line across box represents median, black, filled triangle represents the mean, whiskers in the boxplots represent the maximum and minimum range of the data. Positive values indicate 1-hourly meteorological simulation was lower than the defined scenario. Numbers at the bottom of graphs represent the mean annual biomass for hourly meteorological resolution in units of  $\text{mg C m}^{-2}$ . DIC = dissolved inorganic carbon, P=phytoplankton, Z = zooplankton, B = Bacteria, POC = particulate organic carbon, DOC = dissolved organic carbon, ben. = benthic.

phytoplankton, zooplankton, and particulate organic carbon (POC) pools generally decrease with lowering resolution of meteorological forcing. All other carbon reservoirs at L4 show no obvious trend to changing meteorological resolution. In contrast, at CCS, carbon stocks increase with lower meteorological resolution in every year between 2010 and 2015 in all pools except for phytoplankton, DIC, and benthic bacteria. While both the mean and median of phytoplankton and benthic bacterial biomasses increase with lower meteorological forcing, there are some years where lower biomasses occur relative to the hourly forcing scenario.

### 3.7. Response of Carbon Fluxes

At L4, decreased meteorological resolution generally results in a lower GPP, reflecting the reduction in phytoplankton biomass (Figure 7). In contrast, at CCS, there is an annual increase in GPP associated with a reduction in resolution of meteorological forcing despite the high variability in changes of phytoplankton biomass at this site (Figure 7). The simulated increase in the mass of DOC at both sites (Figure 6) is reflected in the increased production of DOC from phytoplankton by excretion and cell lysis with lowering meteorological resolution. This positive relationship between the release of DOC by phytoplankton and lower meteorological resolution is greatest during spring, while a negative relationship is observed during summer at both sites.

The greater production of DOC from phytoplankton in the 6 hr resolution compared to the hourly simulation at both L4 and CCS is further highlighted in Figure 8. Both stations show an enhanced microbial loop in the 6 hr scenario with greater transfer of carbon between phytoplankton, DOC, bacteria, and DIC. The

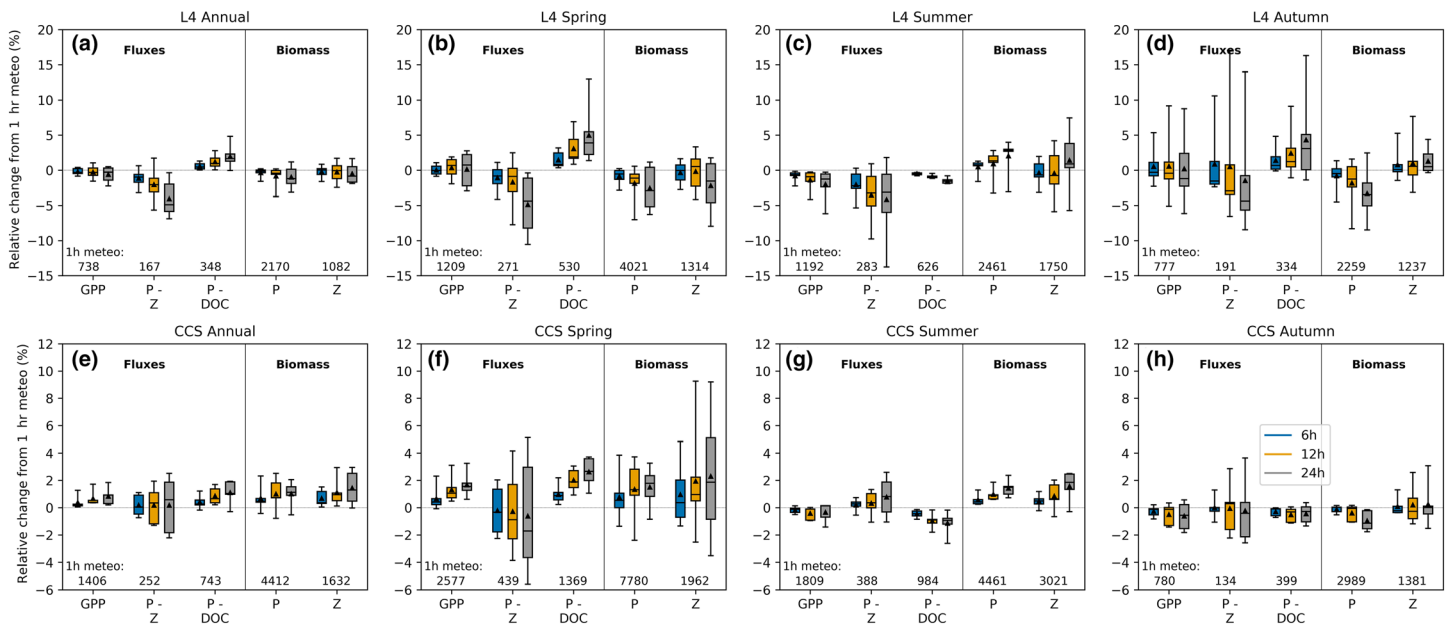


**Figure 7.** Impact of meteorological forcing on the depth-integrated, mean fluxes controlling phytoplankton and zooplankton biomass for each year over 2010–2015, shown as the percentage change between the 6-, 12-, and 24-hourly meteorological forcing and the hourly meteorological forcing simulation at L4 (a–d) and CCS (e–h). Seasons correspond to the days of the year given in Table S3. Positive values indicate 1-hourly meteorological simulation was lower than the defined scenario. Line across box represents median, black, filled triangle represents the mean, whiskers in the boxplots represent the maximum and minimum range of the data. Note difference in scales between stations. Numbers on bottom of graph indicate the result of the 1 h meteorological forcing simulation (fluxes:  $\text{mg C m}^{-2} \text{ day}^{-1}$ , biomass:  $\text{mg C m}^{-2}$ ). GPP = gross primary production, P-Z = phytoplankton to zooplankton flux, P-DOC = phytoplankton to dissolved organic carbon flux, P = phytoplankton, and Z = zooplankton.

enhanced microbial loop at both sites occurs despite opposing trends in both GPP and zooplankton predation of phytoplankton between sites. The same trends are observed in the 12-hourly and 24-hourly meteorological resolution scenarios (results not shown).

Changes in phytoplankton phenology also impact the flux of POC to the sediment (Figure S6). At L4, deposition of POC is marginally earlier in the reduced resolution scenarios relative to the hourly simulation. A reduction in the peak depositional flux of POC by up to 5% also occurs during spring with lowering meteorological resolution, while a slight enhancement of POC deposition occurs in autumn. In contrast, at CCS an enhanced and earlier depositional flux of POC occurs during the spring bloom as the meteorological resolution is reduced although there is little difference throughout the rest of the year.

#### 4. Discussion

Phytoplankton phenology is known to be strongly impacted by meteorological variables, particularly wind and solar irradiance. The timing of spring and autumn phytoplankton blooms have consequences that cascade through the food web (Edwards & Richardson, 2004) and have been shown to affect fish stocks and spawning, copepod reproduction and shrimp survival (Kodama et al., 2018; Leaf & Friedland, 2014; Marrari et al., 2019; Platt et al., 2003; Richards et al., 2016). If high-resolution meteorological data is not available, the ability of hydrodynamic-ecosystem models to capture the impact of short-term fluctuations in wind stress, light availability and other key meteorological variables on bloom phenology and carbon cycling is limited. Here we show that these short-term fluctuations contribute to the amount of energy available within the water column and thus influence both physical and ecological dynamics within ocean models. Our study is designed to highlight the potential impacts of changing meteorological forcing resolution on ecosystem dynamics. This work provides insight into which variables and processes the phytoplankton blooms at both sites are sensitive to as discussed below, but it is not designed to determine which factors trigger the phytoplankton blooms at both sites.

An idealized conceptual model explaining the role of meteorological resolution and ecosystem implications is created from our results (Figure 9). A coarsening in meteorological resolution misses high intensity wind

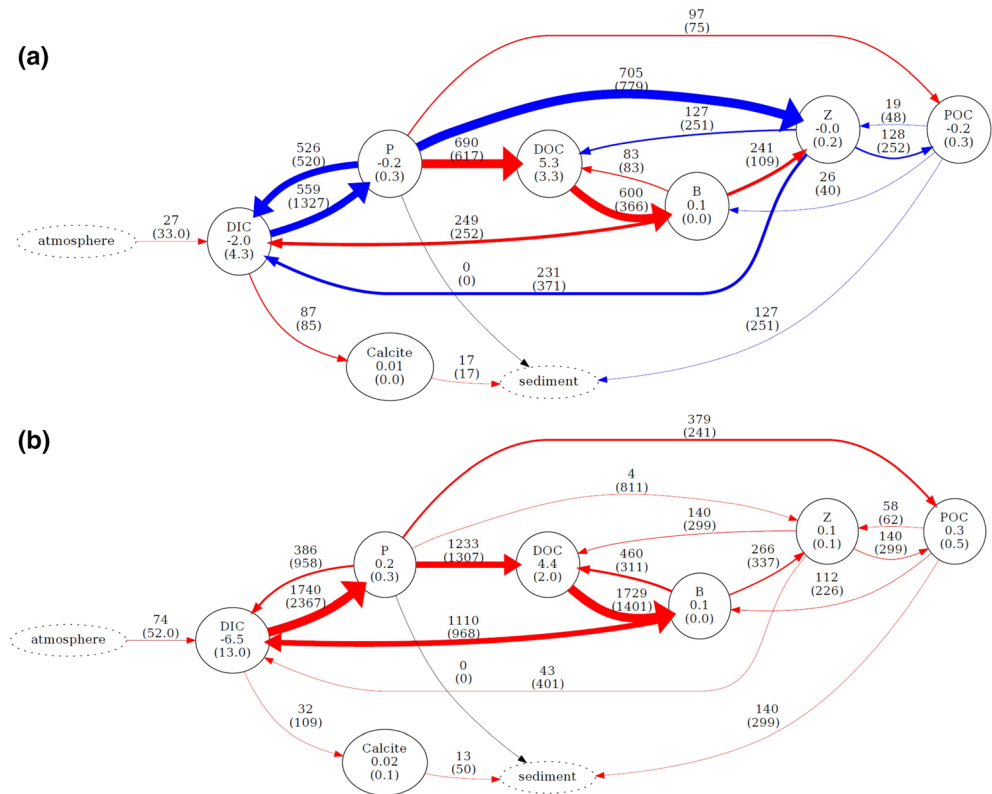


**Figure 8.** Flow diagram indicating mean differences in carbon reservoirs and fluxes between 2010 and 2015 between the 6-hourly meteorological resolution scenario and hourly simulation for stations (a) L4 and (b) CCS. Numbers in brackets represent the standard deviation of annual fluxes and reservoirs. Width of arrows is proportional to size of absolute flux, red indicates an increase in the 6-hourly forcing relative to the hourly while blue indicates a decrease. DIC = dissolved inorganic carbon, P = phytoplankton, Z = zooplankton, B = Bacteria, POC = particulate organic carbon, DOC = dissolved organic carbon. Reservoir units:  $\text{mg C m}^{-3}$ ; flux units:  $\text{mg C m}^{-2} \text{yr}^{-1}$ .

events and thus produces less turbulent kinetic energy within the water column resulting in a longer period of stratification, during which phytoplankton cells remain near the surface and are not mixed down to non-viable, low-light depths. Consequently, the growing season is longer, with the spring bloom starting earlier and the autumn bloom often terminating later. In addition to the bloom starting earlier, changes in wind stress have contrasting impacts on phytoplankton biomass due to (1) reduced winds mix fewer nutrients across the nutricline leading to weaker spring blooms or (2) the phytoplankton bloom lasts longer with lower meteorological resolution as increased winds can cause an earlier cessation of the phytoplankton bloom by mixing the phytoplankton out of the photic zone (Follows & Dutkiewicz, 2002; Waniek, 2003). The balance between enhanced winds mixing nutrients across the nutricline, alleviating nutrient stress, and mixing phytoplankton out of the photic zone contributes to the direction of change in GPP to meteorological forcing in addition to the changes in the length of the growing season. Consequently, implications for ecosystem function are site dependent and is discussed further in section 4.2. In this study, an enhanced microbial loop occurs at both sites with coarsening meteorological resolution although different mechanisms drive the enhancement.

#### 4.1. Impacts of Wind Stress on Phytoplankton Phenology

A coarsening of meteorological forcing resolution causes decreased wind stress on the ocean surface. Our results showing an earlier spring phytoplankton bloom under decreased wind stress are unsurprising given the earlier onset of stratification (Figure 4) and are consistent with the critical turbulence hypothesis of Taylor and Ferrari (2011) and results of Chiswell (2011) and Vikebø et al. (2019) who link the timing of the spring bloom to wind-driven processes. The earlier phytoplankton bloom with decreased wind stress matches trends observed in other shallow systems such as in the European Shelf (González Taboada &

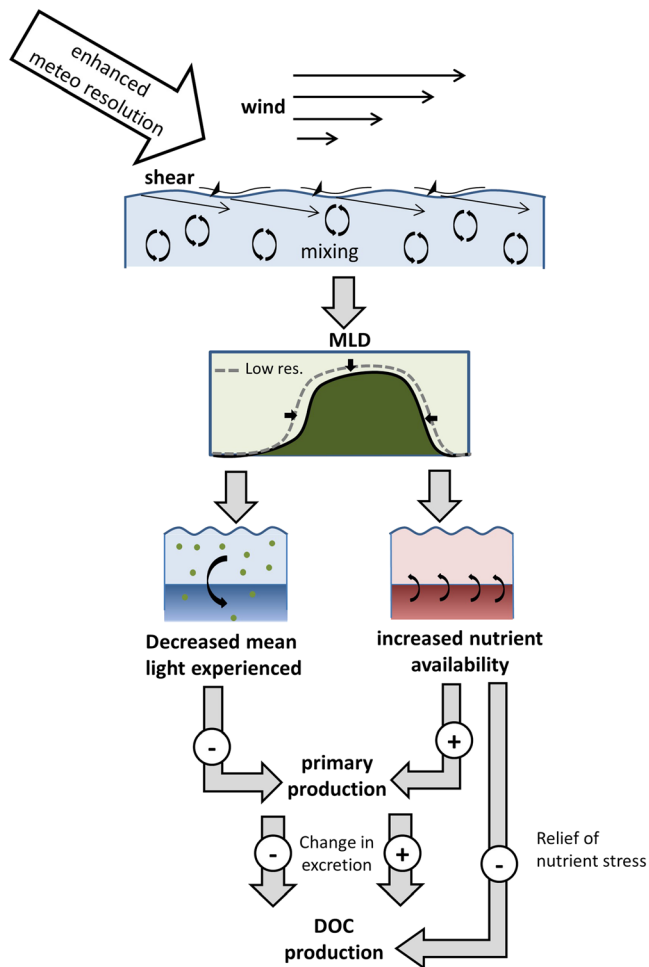


**Figure 9.** Conceptual model highlighting the impact of enhancing the meteorological resolution, and thus wind stress on primary and dissolved organic carbon (DOC) production. Increased mixing results in more phytoplankton mixed out of the photic zone, decreasing the average amount of light experienced by phytoplankton, and increased nutrients being mixed across the nutricline into the photic zone. Note changes in mixed layer depth (MLD) are exaggerated for purpose of this illustration.

more time to respond to changes in phytoplankton biomass. Hence, lower phytoplankton biomass and greater primary production, would occur, in addition to greater zooplankton biomass. This mechanism appears to arise during 2014 at CCS and 2015 at L4 when there is a lower peak magnitude of phytoplankton biomass and higher peak zooplankton in the hourly simulation compared to the 24-hourly scenario (Figure S5b), although the peak magnitude of GPP is also lower during these years. In all other years where a decrease in phytoplankton biomass occurs in the hourly simulation relative to the scenarios (i.e., 2012 L4 and CCS; Figures S5a and S5b), a lower peak in zooplankton also occurs.

In addition to changing phytoplankton bloom length, interannual changes in meteorological variables have also been linked to an increase in the length of the growing season. Increasing delays between spring and autumn blooms have been observed in the temperate North Atlantic, and are attributed to enhanced stratification due to the warming of the ocean (González Taboada & Anadón, 2014). Here, we show that differences in wind stress can also prolong the period of stratification and consequently the length of the growing season (Figure 4). Wihsgott et al. (2019) determine that wind stress is important in controlling the breakdown of stratification and hence the timing of the autumn bloom at CCS. During 2014 and 2015 at CCS, wind stress was predicted to be responsible for controlling the MLD 53% of the time, increasing to more than 60% during the period of the autumn bloom (Wihsgott et al., 2019). Similar to the spring

Anadón, 2014), Central Cantabrian Sea (Álvarez et al., 2009), and Baltic Sea (Groetsch et al., 2016). However, Barnes et al. (2015) predict that the peak amplitude of the spring microphytoplankton bloom at L4 is later in years when there is reduced wind although this tends to coincide with either warmer sea surface temperatures or low salinity. A similar trend for phytoplankton bloom initiation is also shown by Krug et al. (2018) in the shelf slope system off the south west Iberian peninsula. Both studies hypothesized that reduced winds decreased the availability of winter nutrients for phytoplankton due to enhanced stratification and reduced mixing. The differences between our results and those predicted by Barnes et al. are likely due to differences in methods: Barnes et al. average wind speeds at L4 on a seasonal to annual scale so their results are not directly comparable to what we present here.

The earlier start of the phytoplankton bloom at CCS with decreasing winds is also in contrast to that predicted by Henson et al. (2009). Using a combination of satellite data and model predictions, these authors indicate that bloom timing is delayed during both positive and negative phases of the North Atlantic Oscillation (NAO), which cause enhanced and decreased winds, respectively, at the approximate location of the CCS study site. However, Henson et al. (2009) use a different set of criteria to define the start of the bloom and predict the onset at CCS 1–2 months earlier than we report here. Earlier in the season, phytoplankton phenology could be more sensitive to other factors associated with the NAO such as light or sea surface temperature, which may offset the changes associated with wind stress that we have found.

Earlier phytoplankton blooms which are (at least partially) attributed to a decrease in wind stress are often longer and weaker than phytoplankton blooms that occur later in the season (González Taboada & Anadón, 2014; Groetsch et al., 2016) although, Krug et al. (2018) found the opposite trend on the coastal shelf off the south west Iberian peninsula. Our results also suggest a longer bloom with decreased wind stress due to both an earlier start and later finish to the bloom (Figure 5). In addition, although there is a tendency at both sites toward a diminished bloom magnitude when the bloom starts earlier this does not always happen. In cases where the wind disrupts the formation of stratification, Waniek (2003) predicts that zooplankton biomass will increase relative to years with uninterrupted formation of stratification, due to having



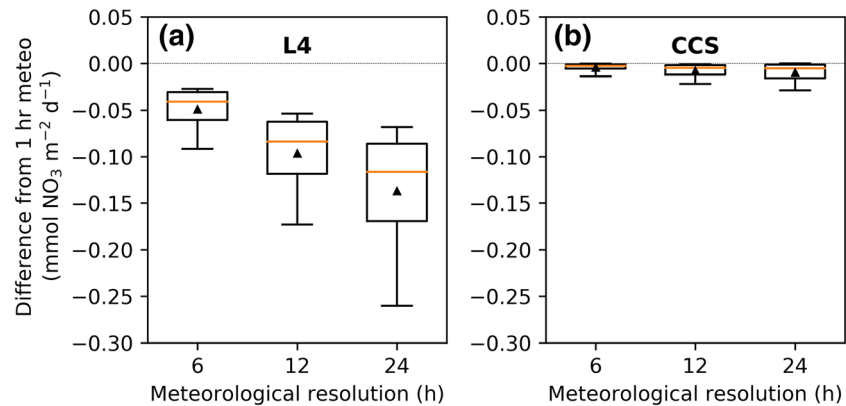


**Figure 10.** Vertical diffusive flux of nitrate within the mixed layer (7.5 m L4; 20 m CCS) during summer shown as the difference between 6-, 12-, and 24-hourly meteorological forcing and the hourly meteorological forcing simulation at L4 (a) and CCS (b) for years 2010–2015. Line across box represents median, black, filled triangle represents the mean, whiskers in the boxplots represent the maximum and minimum range of the data.

bloom, our results suggest that increased wind stress can enhance the peak magnitude of phytoplankton biomass during autumn at both CCS and L4 (i.e., in 2012, CCS, 2013, L4; Figures S5e and S5f) but also terminate the bloom earlier (2011, L4). Overall, this leads to enhanced phytoplankton biomass in the hourly simulation compared to the reduced resolution scenarios at both stations during autumn (Figure 7).

The timing and magnitude of the autumn bloom, particularly across the outer shelf immediately before a period of net off-shelf transport during the winter (Ruiz-Castillo et al., 2019), could affect the amount of carbon annually exported off-shelf (Wihsgott et al., 2019). Although not captured by the 1-D model, wind stress plays an important role in seasonal shelf-scale circulation (Ruiz-Castillo et al., 2018) and can advance (delay) the onset (breakdown) of stratification by ~1 week via a horizontal salinity straining mechanism, with corresponding adjustments to the spring and autumn bloom timings (Ruiz-Castillo et al., 2019). The changes in bloom timing reported here that result from differing temporal resolutions of the wind stress forcing are of the same magnitude.

#### 4.2. What Drives the Enhanced Microbial Loop?

An enhanced microbial loop occurs at both sites with lowering meteorological resolution (Figure 8). However, the impact on the ecosystem structure and nutrient dynamics due to the change in stratification is different between the two sites, despite similarities in the phenology. A key driver of the microbial loop is the change in DOC production. DOC production provides food for bacteria, which enhances remineralization of carbon back to DIC. Extracellular release of DOC by phytoplankton is the main source of DOC to marine systems (Borchard & Engel, 2015). Extracellular release may occur through passive diffusion of low molecular weight compounds across cell membranes (Bjornsen, 1988) or through active release of DOC by exudation (Fogg, 1983) which has been shown to be enhanced by environmental stress such as nutrient limitation (Borchard & Engel, 2015; Goldman et al., 1992; Mühlenbruch et al., 2018; Smith et al., 1998). Within ERSEM, DOC is released by phytoplankton as a fixed portion of GPP through excretion (Butenschön et al., 2016). In addition, phytoplankton within ERSEM release higher proportions of DOC when undergoing nutrient stress through cell lysis and excretion.

We propose that different mechanisms are driving the enhanced microbial loop at each site reflecting the site-specific response of GPP, phytoplankton and zooplankton to the meteorological forcing. The small increase in GPP at CCS with lowering meteorological forcing resolution likely reflects the longer growing season due to the increased amount of time that the water column is stratified (Figure 4). The higher GPP could further reflect less turbulent conditions and thus a greater time that phytoplankton remain in the photic zone. The greater GPP in spring as meteorological resolution decreases (Figure 7) supports both these hypotheses. In contrast, at L4 there is a weak trend toward a decreasing GPP on an annual scale with coarsening meteorological resolution which reflects the lower phytoplankton biomass in the scenarios (Figure 7). The decreasing trend is greatest during summer and likely reflects the weaker flux of nutrients across the nutricline during this time period (Figure 10a) as there is reduced kinetic energy within

the water column. This mechanism is much weaker at CCS (Figure 10b) as there the nutricline is positioned at greater depth, out of reach of the turbulence produced by surface wind stress. Thus, greater wind stress is required at CCS to break down stratification up to the depth of the nutricline. Lower GPP at L4 in the scenarios may also be driven by the thinner mixed layer resulting in a reduction in the total mass of nutrients within the mixed layer available for phytoplankton growth (Figures 4 and S5c). This last process is hypothesized to be important for bloom timing in nutrient limited subtropical seas (Henson et al., 2009).

The contrasting trends in GPP at L4 and CCS highlight the role that resource limitation plays in the response of a system to external variables. The spring bloom at L4 ultimately becomes limited by nitrate concentrations, which remain low within surface waters throughout the summer (Smyth et al., 2010). At CCS the spring bloom is typically both light and nitrate limited with summer phytoplankton growth nitrate limited and the autumn bloom light limited (Poulton et al., 2018). This is confirmed in the model by the light and nutrient limitation factors which show a similar trend between the two sites for nutrients in the hourly simulation and an enhanced light limitation at CCS compared to L4 (Figure S7). Light limitation appears more important in controlling the response of the ecosystem to changes in meteorological forcing at CCS than nutrient limitation due to the correlation between growing season and GPP and the relatively strong stratification in summer reducing the impact of turbulent mixing. In addition, the variation in phytoplankton biomass compared to trends in GPP further suggests, at least in some years, top-down control on phytoplankton by zooplankton. This highlights the potential mismatch within the plankton community to changes (Edwards & Richardson, 2004). Indeed, zooplankton displays the highest relative change out of all the pelagic carbon reservoirs to meteorological forcing at CCS. Although not directly included in ERSEM, a delayed phytoplankton bloom start can further limit phytoplankton biomass due to an enhanced zooplankton population as a result of reproduction (Henson et al., 2009).

The fact that the two different sites, one light limited and one nutrient limited, both show increased DOC concentrations with lower meteorological resolution is directly linked to the multiple pathways for DOC formation in ERSEM. The increased GPP at CCS results in greater release of DOC by phytoplankton, as indicated by the similar trend in the production of DOC by phytoplankton and GPP. In contrast at L4, phytoplankton become more nutrient stressed as resolution of meteorological forcing reduces (Figures S7 and S8), which is highlighted by the differing trends between the creation of DOC by phytoplankton and GPP, during spring, autumn and on an annual scale (Figure 7). The increased nutrient stress with lowering meteorological resolution is likely due to a combination of the decrease in mixing which then reduces the amount of nutrients available for phytoplankton growth during the spring and autumn blooms, and the longer growing season with coarsening meteorological resolution resulting in a longer period of nutrient stress and thus increases the stress induced DOC production. The enhanced DOC concentrations intensifies the microbial loop, stimulating bacterial production and hence cycling of carbon back to DIC in the lower meteorological resolution simulations (Figure 8).

### 4.3. Increasing Meteorological Resolution in Hydrodynamic Ecosystem Models

The recent release of the ERA5 reanalysis product (C3S, 2017) will result in increasingly higher resolution of meteorological forcing being used in ocean models. Little consideration may be made on how this could impact ecosystem dynamics. Our results show that switching the resolution of meteorological forcing from a dataset such as ERA-Interim (Dee et al., 2011), which provides 6-hourly analysis for meteorological data, to ERA5 could impact both phytoplankton phenology and ecosystem structure. The change in the timing of the start of the bloom of up to 6 days due to resolution of meteorological forcing is substantial given that it is on the same order of magnitude as the variability of the start date of phytoplankton blooms observed in the North Sea and that of the response of benthic communities to depositional carbon fluxes (Sharples et al., 2006; Lessin et al., 2019) in addition to the timescale of forecasts made by operational models. Large variability also exists in the response of phytoplankton phenology and ecosystem dynamics to meteorological forcing with some years showing little change. Thus, changing the resolution of meteorological forcing enhances the predicted variability in timing of blooms in addition to the changes in the microbial loop and depositional fluxes to the sea floor.

We have investigated the impact that wind in a 1-D model has on physical and biogeochemical dynamics. The impacts in 3-D may be greater than presented here as the spatial resolution of the horizontal grid

from ERA-Interim to ERA 5 improves from 79 to 31 km adding further fluctuations in wind stress to the surface water. In addition, hourly light and cloud cover data will also result in changes between ERA5 and ERA-Interim. Here, we purposefully kept net shortwave radiation constant in all scenarios as the effect of changes in incoming shortwave radiation as a result of switching from ERA5 to ERA-Interim are likely to be model specific, depending on the model formulations for light. Changes in bias in the ERA-Interim and ERA5 data sets, for example, the higher precipitation rates over Europe in ERA5 than ERA-Interim (ECMWF/C3S/CAMS, 2017), should also be considered when changing meteorological forcing, but are beyond the scope of this study.

There may also be projects when time averaged meteorological variables (i.e., Blackford, 2002; Ridderinkhof, 1992) are used rather than instantaneous values. Time averaging meteorological variables rather than subsampling, produces greater changes than observed here. Running the model with daily (24 hr) averaged data, further dampens the variability in meteorological inputs reducing the wind stress acting on sea surface resulting in larger changes in phytoplankton phenology and ecosystem dynamics than what we predict in the 24 hr subsampled scenario (results not shown).

## 5. Conclusion

This study investigates the response of shelf-sea ecosystems to the resolution of meteorological forcing in hydrodynamic-ecosystem models. This is especially important given the increased availability of hourly datasets such as the ERA5 and NCEP Climate Forecast System products. In general, a higher temporal resolution of meteorological forcing results in greater mixing within the water column with a later development of the surface mixed layer in spring and earlier breakdown in autumn. This produces a shorter growing season and later start to the phytoplankton bloom, which directly impacts higher trophic levels within the ecosystem, and at CCS, weakens deposition of POC to the sea floor during spring. The strength of the microbial loop at both sites is reduced: At the coastal L4 station this is a consequence of the relief of nutrient stress resulting in less DOC expelled by phytoplankton, at the offshore CCS station, this is a consequence of the decrease in GPP due to the reduced growing season.

Our results show that it is important to consider the impact that changes in meteorological forcing of coupled hydrodynamic-ecosystem models will have on interpreting physical and ecosystem dynamics. Although this work only includes two sites on shelf seas, we believe that our work can be extrapolated to other sites globally and other model setups. We envision that the sites, which will show the biggest response to meteorological forcing, are those that are seasonally or intermittently stratified, similar to the ones studied here. These sites represent approximately 44% of the surface area of the North Sea (van Leeuwen et al., 2015). Permanently mixed sites are unlikely to show any strong impact to changes in meteorological forcing resolution, while permanently stratified sites might show a small response to meteorological forcing. The conceptual model that we present can be used to guide researchers on expected outcomes using their knowledge of stratification of an individual site, resource limitation status and model design (i.e., whether there is a stress release mechanism for DOC). The main effect of changing the meteorological forcing in this study was to increase the variability of winds, consequently adding more energy into the water column. A main limitation of our study is that changes in the frequency of prescribed shortwave radiation, or cloud cover, were not investigated. The ecosystem response to such changes are likely to be dependent on individual model formulations for light, which should also be considered when switching meteorological forcing. Thus, recalibration of models may be required when switching meteorological forcing, which may give new insights to ecosystem dynamics.

## Data Availability Statement

All observational data used in this work can be downloaded from [www.bodc.ac.uk](http://www.bodc.ac.uk) and is referenced in the main text, except for the following dois corresponding to the CCS CTD data collected during the cruises mentioned in section 2.1 of the main text: doi:10/c4mj, doi:10/c4pk, doi:10/c4mk, doi:10/c4ph, doi:10/c4pk, doi:10/c4pj, doi:10/c4pf, and doi:10/c4pg. The model configurations used in this paper to run GOTM-FABM-ERSEM, links to download the model code, and nc files containing the model results can be downloaded from [https://zenodo.org/record/3712237#.Xq\\_UWqhKjD4](https://zenodo.org/record/3712237#.Xq_UWqhKjD4) website.

**Acknowledgments**

This work was supported by NERC-funded project, Combining Autonomous observations and Models for Predicting and Understanding Shelf seas (CAMPUS; NE/R006849/1 and NE/R006822/2) and the NERC single center national capability program—Climate Linked Atlantic Sector Science (NE/R015953/1). We thank Jason Holt, Lewis Drysdale, and the modeling group at PML for useful discussions on this work.

**References**

Álvarez, E., Nogueira, E., Acuña, J. L., Lopez-Álvarez, M., & Sostres, J. A. (2009). Short-term dynamics of late-winter phytoplankton blooms in a temperate ecosystem (Central Cantabrian Sea, Southern Bay of Biscay). *Journal of Plankton Research*, *31*, 601–617. <https://doi.org/10.1093/plankt/fbp012>

Aveytua-Alcázar, L., Camacho-Ibar, V. F., Souza, A. J., Allen, J. I., & Torres, R. (2008). Modelling *Zostera marina* and *Ulva* spp. in a coastal lagoon. *Ecological Modelling*, *218*(3–4), 354–366. <https://doi.org/10.1016/j.ecolmodel.2008.07.019>

Backhaus, J. (1985). A three dimensional model for the simulation of shelf sea dynamics. *Deutsche Hydrografische Zeitschrift*, *38*(4), 165–187. <https://doi.org/10.1007/BF02328975>

Barnes, M. K., Tilstone, G. H., Suggett, D. J., Widdicombe, C. E., Bruun, J., Martínez-Vicente, V., & Smyth, T. J. (2015). Temporal variability in total, micro- and nano-phytoplankton primary production at a coastal site in the Western English Channel. *Progress in Oceanography*, *137*, 470–483. <https://doi.org/10.1016/j.pocean.2015.04.017>

Bauer, J. E., Cai, W. J., Raymond, P. A., Bianchi, T. S., Hopkinson, C. S., & Regnier, P. A. G. (2013). The changing carbon cycle of the coastal ocean. *Nature*, *504*(7478), 61–70. <https://doi.org/10.1038/nature12857>

Behrenfeld, M. J. (2010). Abandoning Sverdrup's Critical Depth Hypothesis on phytoplankton blooms. *Ecology*, *91*(4), 977–989. <https://doi.org/10.1890/09-1207.1>

Behrenfeld, M. J., Doney, S. C., Lima, I., Boss, E. S., & Siegel, D. A. (2013). Annual cycles of ecological disturbance and recovery underlying the subarctic Atlantic spring plankton bloom. *Global Biogeochemical Cycles*, *27*, 1291–1293. <https://doi.org/10.1002/2013GB004681>

Bjornsen, P. K. (1988). Phytoplankton exudation of organic matter: Why do healthy cells do it? *Limnology and Oceanography*, *33*(1), 151–154. <https://doi.org/10.4319/lo.1988.33.1.0151>

Blackford, J. C. (2002). The influence of microphytobenthos on the Northern Adriatic ecosystem: A modelling study. *Estuarine, Coastal and Shelf Science*, *55*(1), 109–123. <https://doi.org/10.1006/ecs.2001.0890>

Blackford, J. C., & Burkill, P. H. (2002). Planktonic community structure and carbon cycling in the Arabian Sea as a result of monsoonal forcing: The application of a generic model. *Journal of Marine Systems*, *36*(3–4), 239–267. [https://doi.org/10.1016/S0924-7963\(02\)00182-3](https://doi.org/10.1016/S0924-7963(02)00182-3)

Borchard, C., & Engel, A. (2015). Size-fractionated dissolved primary production and carbohydrate composition of the coccolithophore *Emiliania huxleyi*. *Biogeosciences*, *12*(4), 1271–1284. <https://doi.org/10.5194/bg-12-1271-2015>

Bruggeman, J., & Bolding, K. (2014). A general Framework for Aquatic Biogeochemical Models. *Environmental Modelling and Software*, *61*, 249–265. <https://doi.org/10.1016/j.envsoft.2014.04.002>

Burchard, H., Bolding, H., & Villareal, M. (1999). GOTM: A general ocean turbulence model. In *Theory, applications and test cases* (Technical Report EUR 18745 EN). European Commission.

Butenschön, M., Clark, J., Aldridge, J. N., Allen, J. I., Artioli, Y., Blackford, J., et al. (2016). ERSEM 15.06: A generic model for marine biogeochemistry and the ecosystem dynamics of the lower trophic levels. *Geoscientific Model Development*, *9*(4), 1293–1339. <https://doi.org/10.5194/gmd-9-1293-2016>

C3S, (Copernicus Climate Change Service) (2017). ERA5: Fifth generation of ECMWF atmospheric reanalyses of the global climate. Copernicus Climate Change Service Climate Data Store (CDS). Retrieved from <https://cds.climate.copernicus.eu/cdsapp#!/home>

Cazenave, P. W., Torres, R., & Allen, J. I. (2016). Unstructured grid modelling of offshore wind farm impacts on seasonally stratified shelf seas. *Progress in Oceanography*, *145*, 25–41. <https://doi.org/10.1016/j.pocean.2016.04.004>

Chiswell, S. M. (2011). Annual cycles and spring blooms in phytoplankton: Don't abandon Sverdrup completely. *Marine Ecology Progress Series*, *443*, 39–50. <https://doi.org/10.3354/meps09453>

de Boyer Montégut, C., Madec, G., Fischer, A. S., Lazar, A., & Iudicone, D. (2004). Mixed layer depth over the global ocean: An examination of profile data and a profile-based climatology. *Journal of Geophysical Research*, *109*, C12003. <https://doi.org/10.1029/2004JC002378>

Dee, D. P., Uppala, S. M., Simmons, A. J., Berrisford, P., Poli, P., Kobayashi, S., et al. (2011). The ERA-Interim reanalysis: Configuration and performance of the data assimilation system. *Quarterly Journal of the Royal Meteorological Society*, *137*(656), 553–597. <https://doi.org/10.1002/qj.828>

ECMWF/C3S/CAMS. (2017) Quality of ERA-Interim and comparison with other datasets: Precipitation In European State of the Climate 2017. Retrieved June 4, 2019, from <https://climate.copernicus.eu/quality-era-interim-and-comparison-other-datasets-precipitation>

Edwards, M., & Richardson, A. J. (2004). Impact of climate change on marine pelagic phenology and trophic mismatch. *Nature*, *430*(7002), 881–884. <https://doi.org/10.1038/nature02808>

Fishwick, J. (2018). *CTD profiles (depth, pressure, temperature, salinity, potential temperature, density, fluorescence, transmittance, downwelling PAR, dissolved oxygen concentration) binned to 0.5 m and 0.25 m at sites L4 and E1 in the Western English Channel between January 2002 and December 2015*. UK: British Oceanographic Data Centre, Natural Environment Research Council. <https://doi.org/10.5285/54820666-b5df-266e-e053-6c86abc02283>

Fogg, G. E. (1983). The ecological significance of extracellular products of phytoplankton photosynthesis. *Botanica Marina*, *26*, 3–14.

Follows, M., & Dutkiewicz, S. (2002). Meteorological modulation of the North Atlantic spring bloom. *Deep Sea Research Part II: Topical Studies in Oceanography*, *49*(1–3), 321–344. [https://doi.org/10.1016/S0967-0645\(01\)00105-9](https://doi.org/10.1016/S0967-0645(01)00105-9)

Goldman, J. C., Hansell, D. A., & Dennett, M. R. (1992). Chemical characterization of three large oceanic diatoms: Potential impact on water column chemistry. *Marine Ecology Progress Series*, *88*, 257–270. <https://doi.org/10.3354/meps088257>

González Taboada, F., & Anadón, R. (2014). Seasonality of North Atlantic phytoplankton from space: Impact of environmental forcing on a changing phenology (1998–2012). *Global Change Biology*, *20*(3), 698–712. <https://doi.org/10.1111/gcb.12352>

Groetsch, P. M. M., Simis, S. G. H., Eleveld, M. A., & Peters, S. W. M. (2016). Spring blooms in the Baltic Sea have weakened but lengthened from 2000 to 2014. *Biogeosciences*, *13*(17), 4959–4973. <https://doi.org/10.5194/bg-13-4959-2016>

Henson, S. A., Dunne, J. P., & Sarmiento, J. L. (2009). Decadal variability in North Atlantic phytoplankton blooms. *Journal of Geophysical Research*, *114*, C04013. <https://doi.org/10.1029/2008JC005139>

Holt, J. T., & James, I. D. (2001). An s coordinate density evolving model of the northwest European continental shelf: 1. Model description and density structure. *Journal of Geophysical Research*, *106*(C7), 14015–14034. <https://doi.org/10.1029/2000JC000304>

Hopkins, J., Mountfield, D., Seguro Requejo, I., & Poulton, A. (2019). *CTD profiles (chlorophyll, density, dissolved oxygen concentration, conductivity, optical backscatter, salinity, temperature, transmittance, pressure, down-welling PAR) collected during UK Shelf Sea Biogeochemistry cruise RRS Discovery DY033*. UK: British Oceanographic Data Centre, National Oceanography Centre (NERC). <https://doi.org/10.5285/86532abd-d895-2c4c-e053-6c86abc0db01>

Huisman, J., van Oostveen, P., & Weissing, F. J. (1999). Critical depth and critical turbulence: Two different mechanisms for the development of phytoplankton blooms. *Limnology and Oceanography*, *44*(7), 1781–1787. <https://doi.org/10.4319/lo.1999.44.7.1781>



- Hull, T., Sivyer, D. B., Pearce, D., Greenwood, N., Needham, N., Read, C., & Fitton, E. (2017). *Shelf sea biogeochemistry—CANDYFLOSS SmartBuoy*. UK: CEFAS. <https://doi.org/10.14466/CefasDataHub.37>
- Jolliff, J. K., Kindle, J. C., Shulman, I., Penta, B., Friedrichs, M. A. M., Helber, R., & Arnone, R. A. (2009). Summary diagrams for coupled hydrodynamic-ecosystem model skill assessment. *Journal of Marine Systems*, 76(1–2), 64–82. <https://doi.org/10.1016/j.jmarsys.2008.05.014>
- Kim, H. X., Yoo, S., & Oh, I. S. (2007). Relationship between phytoplankton bloom and wind stress in the sub-polar frontal area of the Japan/East Sea. *Journal of Marine Systems*, 67(3–4), 205–216. <https://doi.org/10.1016/j.jmarsys.2006.05.016>
- Kodama, T., Wagawa, T., Ohshimo, S., Morimoto, H., Iguchi, N., Fukudome, K. I., et al. (2018). Improvement in recruitment of Japanese sardine with delays of the spring phytoplankton bloom in the Sea of Japan. *Fisheries Oceanography*, 27(4), 289–301. <https://doi.org/10.1111/fog.12252>
- Krug, L. A., Platt, T., Sathyendranath, S., & Barbosa, A. B. (2018). Patterns and drivers of phytoplankton phenology off SW Iberia: A phenoregion based perspective. *Progress in Oceanography*, 165, 233–256. <https://doi.org/10.1016/j.poccean.2018.06.010>
- Leaf, R. T., & Friedland, K. D. (2014). Autumn bloom phenology and magnitude influence haddock recruitment on Georges Bank. *ICES Journal of Marine Science*, 71(8), 2017–2025. <https://doi.org/10.1093/icesjms/fsu076>
- Lenhart, H. J., Radach, G., Backhaus, J. O., & Pohlmann, T. (1995). Simulations of the north sea circulation, its variability, and its implementation as hydrodynamical forcing in ERSEM. *Netherlands Journal of Sea Research*, 33(3–4), 271–299. [https://doi.org/10.1016/0077-7579\(95\)90050-0](https://doi.org/10.1016/0077-7579(95)90050-0)
- Lenhart, H. J., Radach, G., & Ruardij, P. (1997). The effects of river input on the ecosystem dynamics in the continental coastal zone of the North Sea using ERSEM. *Journal of Sea Research*, 38(3–4), 249–274. [https://doi.org/10.1016/S1385-1101\(97\)00049-X](https://doi.org/10.1016/S1385-1101(97)00049-X)
- Lessin, G., Bruggeman, J., McNeill, C. L., & Widdicombe, S. (2019). Time scales of benthic macrofaunal response to pelagic production differ between major feeding groups. *Frontiers in Marine Science*, 6, 1–12. <https://doi.org/10.3389/fmars.2019.00015>
- Marrari, M., Macchi, G. J., Santos, B., & Leonarduzzi, E. (2019). Influence of environmental conditions on the reproductive success and recruitment of the Argentine hake *Merluccius hubbsi* (southwestern Atlantic Ocean). *Fisheries Oceanography*, 28(1), 66–81. <https://doi.org/10.1111/fog.12387>
- Mühlenbruch, M., Grossart, H. P., Eigemann, F., & Voss, M. (2018, August 1). Mini-review: Phytoplankton-derived polysaccharides in the marine environment and their interactions with heterotrophic bacteria. *Environmental Microbiology*, 20(8), 2671–2685. <https://doi.org/10.1111/1462-2920.14302>
- Platt, T., Funes-Yaco, C., & Frank, K. T. (2003). Spring algal bloom and larval fish survival. *Marine Ecology*, 423, 398–399.
- Pohlmann, T. (1996a). Calculating the annual cycle of the vertical eddy viscosity in the North Sea with a three-dimensional baroclinic shelf sea circulation model. *Continental Shelf Research*, 16(2), 147–161. [https://doi.org/10.1016/0278-4343\(94\)E0037-M](https://doi.org/10.1016/0278-4343(94)E0037-M)
- Pohlmann, T. (1996b). Predicting the thermocline in a circulation model of the North Sea—Part I: Model description, calibration and verification. *Continental Shelf Research*, 16(2), 131–146. [https://doi.org/10.1016/0278-4343\(95\)90885-s](https://doi.org/10.1016/0278-4343(95)90885-s)
- Poulton, A. J., Davis, C. E., Daniels, C. J., Mayers, K. M. J., Harris, C., Tarran, G. A., et al. (2018). Seasonal phosphorus and carbon dynamics in a temperate shelf sea (Celtic Sea). *Progress in Oceanography*, 177, 101872. <https://doi.org/10.1016/j.poccean.2017.11.001>
- Racault, M.-F., Le Quééré, C., Buitenhuis, E., Sathyendranath, S., & Platt, T. (2012). Phytoplankton phenology in the global ocean. *Ecological Indicators*, 14(1), 152–163. <https://doi.org/10.1016/j.ecolind.2011.07.010>
- Racault, M.-F., Sathyendranath, S., Brewin, R. J. W., Raitsos, D. E., Jackson, T., & Platt, T. (2017). Impact of El Niño variability on oceanic phytoplankton. *Frontiers in Marine Science*, 4(May), 1–15. <https://doi.org/10.3389/fmars.2017.00133>
- Raick, C., Delhez, E. J. M., Soetaert, K., & Grégoire, M. (2005). Study of the seasonal cycle of the biogeochemical processes in the Ligurian Sea using a 1D interdisciplinary model. *Journal of Marine Systems*, 55(3–4), 177–203. <https://doi.org/10.1016/j.jmarsys.2004.09.005>
- Richards, R. A., O'Reilly, J. E., & Hyde, K. J. W. (2016). Use of satellite data to identify critical periods for early life survival of northern shrimp in the Gulf of Maine. *Fisheries Oceanography*, 25(3), 306–319. <https://doi.org/10.1111/fog.12153>
- Ridderinkhof, H. (1992). On the effects of variability in meteorological forcing on the vertical structure of a stratified watercolumn. *Continental Shelf Research*, 12(1), 25–36. [https://doi.org/10.1016/0278-4343\(92\)90004-4](https://doi.org/10.1016/0278-4343(92)90004-4)
- Ruiz-Castillo, E., Sharples, J., & Hopkins, J. (2019). Wind-driven strain extends seasonal stratification. *Geophysical Research Letters*, 46, 13,244–13,252. <https://doi.org/10.1029/2019GL084540>
- Ruiz-Castillo, E., Sharples, J., Hopkins, J., & Woodward, M. (2018). Seasonality in the cross-shelf physical structure of a temperate shelf sea and the implications for nitrate supply. *Progress in Oceanography*, 177, 101985. <https://doi.org/10.1016/j.poccean.2018.07.006>
- Saha, S., Behringer, D., Carolina, N., Chelliah, M., Chen, M., Chen, Y., et al. (2010). The NCEP climate forecast system reanalysis. *Bulletin of the American Meteorological Society*, 91(August), 1015–1058. <https://doi.org/10.1175/2010BAMS3001.1>
- Saha, S., Moorthi, S., Wu, X., Wang, J., Nadiga, S., Tripp, P., et al. (2014). The NCEP climate forecast system version 2. *Journal of Climate*, 27(6), 2185–2208. <https://doi.org/10.1175/JCLI-D-12-00823.1>
- Sapiano, M. R. P., Brown, C. W., Schollaert Uz, S., & Vargas, M. (2012). Establishing a global climatology of marine phytoplankton phenological characteristics. *Journal of Geophysical Research*, 117, C08026. <https://doi.org/10.1029/2012JC007958>
- Sharples, J., Mayor, D. J., Poulton, A. J., Rees, A. P., & Robinson, C. (2019). Shelf Sea Biogeochemistry: Nutrient and carbon cycling in a temperate shelf sea water column. *Progress in Oceanography*, 177, 102182. <https://doi.org/10.1016/j.poccean.2019.102182>
- Sharples, J., Ross, O. N., Scott, B. E., Greenstreet, S. P. R., & Fraser, H. (2006). Inter-annual variability in the timing of stratification and the spring bloom in the North-Western North Sea. *Continental Shelf Research*, 26(6), 733–751. <https://doi.org/10.1016/j.csr.2006.01.011>
- Siddorn, J. R., Allen, J. I., Blackford, J. C., Gilbert, F. J., Holt, J. T., Holt, M. W., et al. (2007). Modelling the hydrodynamics and ecosystem of the North-West European continental shelf for operational oceanography. *Journal of Marine Systems*, 65(1–4), 417–429. <https://doi.org/10.1016/j.jmarsys.2006.01.018>
- Siegel, D. A., Doney, S. C., & Yoder, J. A. (2002). The North Atlantic spring phytoplankton bloom and Sverdrup's critical depth hypothesis. *Science*, 296(5568), 730–733. <https://doi.org/10.1126/science.1069174>
- Simpson, J. H., Crisp, D. J., & Hearn, C. (1981). The shelf-sea fronts: Implications of their existence and behaviour [and discussion]. *Philosophical Transactions of the Royal Society A: Mathematical, Physical and Engineering Sciences*, 302(1472), 531–546. <https://doi.org/10.1098/rsta.1981.0181>
- Smith, W. O. Jr., Carlson, C. A., Ducklow, H. W., & Hansell, D. A. (1998). Growth dynamics of Phaeocystis Antarctica-dominated plankton assemblages from the Ross Sea. *Marine Ecology Progress Series*, 168.
- Smyth, T., Atkinson, A., Widdicombe, S., Frost, M., Allen, I., Fishwick, J., et al. (2015). The Western Channel Observatory. *Progress in Oceanography*, 137, 335–341. <https://doi.org/10.1016/j.poccean.2015.05.020>
- Smyth, T. J., Allen, I., Atkinson, A., Bruun, J. T., Harmer, R. A., Pingree, R. D., et al. (2014). Ocean net heat flux influences seasonal to interannual patterns of plankton abundance. *PLoS ONE*, 9(6), e98709. <https://doi.org/10.1371/journal.pone.0098709>



- Smyth, T. J., Fishwick, J. R., al-Moosawi, L., Cummings, D. G., Harris, C., Kitidis, V., et al. (2010). A broad spatio-temporal view of the Western English Channel observatory. *Journal of Plankton Research*, 32(5), 585–601. <https://doi.org/10.1093/plankt/fbp128>
- Sverdrup, H. U. (1953). On conditions for the vernal blooming of phytoplankton. *ICES Journal of Marine Science*, 18(3), 287–295. <https://doi.org/10.1093/icesjms/18.3.287>
- Taylor, J. R., & Ferrari, R. (2011). Shutdown of turbulent convection as a new criterion for the onset of spring phytoplankton blooms. *Limnology and Oceanography*, 56(6), 2293–2307. <https://doi.org/10.4319/lo.2011.56.6.2293>
- Ueyama, R., & Monger, B. C. (2005). Wind-induced modulation of seasonal phytoplankton blooms in the North Atlantic derived from satellite observations. *Limnology and Oceanography*, 50(6), 1820–1829. <https://doi.org/10.4319/lo.2005.50.6.1820>
- van Leeuwen, S., Tett, P., Mills, D., & Van Der Molen, J. (2015). Journal of geophysical research: Oceans. *Journal of Geophysical Research: Oceans*, 120, 4670–4686. <https://doi.org/10.1002/2014JC010485>
- Vichi, M., Zavatarelli, M., & Pinardi, N. (1998). Seasonal modulation of microbially mediated carbon fluxes in the northern Adriatic Sea—A model study. *Fisheries Oceanography*, 7(3-4), 182–190. <https://doi.org/10.1046/j.1365-2419.1998.00082.x>
- Vikebo, F. B., Strand, K. O., & Sundby, S. (2019). Wind intensity is key to phytoplankton spring bloom under climate change. *Frontiers in Marine Science*, 6(August), 1–9. <https://doi.org/10.3389/fmars.2019.00518>
- Waniek, J. J. (2003). The role of physical forcing in initiation of spring blooms in the northeast Atlantic. *Journal of Marine Systems*, 39(1–2), 57–82. [https://doi.org/10.1016/S0924-7963\(02\)00248-8](https://doi.org/10.1016/S0924-7963(02)00248-8)
- Wihsgott, J., Hopkins, J., Sharples, J., Jones, E., & Balfour, C. A. (2016). *Long-term mooring observations of full depth water column structure spanning 17 months, collected in a temperate shelf sea (Celtic Sea)*. UK: British Oceanographic Data Centre, Natural Environment Research Council. <https://doi.org/10.5285/389fe406-ebd9-74f1-e053-6c86abc032a4>
- Wihsgott, J., Sharples, J., Hopkins, J. E., Woodward, E. M. S., Hull, T., Greenwood, N., & Sivyer, D. B. (2019). Observations of vertical mixing in autumn and its effect on the autumn phytoplankton bloom. *Progress in Oceanography*, 177, 102059. <https://doi.org/10.1016/j.pcean.2019.01.001>
- Woodward, E. M. S. (2016). *Discrete inorganic nutrient samples collected from the Celtic Sea during RRS Discovery cruise DY026B in August 2014*. UK: British Oceanographic Data Centre, Natural Environment Research Council. <https://doi.org/10.5285/2eb8d803-8823-1e6f-e053-6c86abc052a6>
- Woodward, E., & Harris, C. (2019). *Nutrient concentration profiles from long term time series at Station L4 in the Western English Channel from 2000 to 2017*. UK: British Oceanographic Data Centre, National Oceanography Centre (NERC). <https://doi.org/10.5285/7f7f661b-29c4-4a95-e053-6c86abc05200>
- Woodward, M. (2016). *Discrete inorganic nutrient samples collected from the Celtic Sea and English Channel during RRS James Cook cruise JC105 in June 2014*. UK: British Oceanographic Data Centre, Natural Environment Research Council. <https://doi.org/10.5285/2eb8d803-8822-1e6f-e053-6c86abc052a6>
- Yamada, K., & Ishizaka, J. (2006). Estimation of interdecadal change of spring bloom timing, in the case of the Japan Sea. *Geophysical Research Letters*, 33, L02608. <https://doi.org/10.1029/2005GL024792>